ORIGINAL ARTICLE

Aspects of 3D rotating hybrid CNT flow for a convective exponentially stretched surface

T. Hayat[1] · S. Nadeem[1] · A. U. Khan[1]

Abstract

To enhance the heat transfer properties within the flow, a newly discovered idea of hybrid nanofluid has been activated. This paper investigates the effect of 3D rotating CNT hybrid nanofluid with magnetic field over a convectively heated and exponentially stretching surface. Two various types of liquids, in particular hybrid nanofluid (SWCNT-MWCNT/Water) and nanofluid (SWCNT-Water) are considered in the present study. Newly demonstrated thermophysical properties are considered. The impacts of different physical parameters on hybrid flow are displayed and discussed briefly. It is observed that the use of hybrid nanofluid would give better heat transfer performance than nanofluid. By choosing different and appropriate nanoparticles' proportions in hybrid nanofluid, the desired heat transfer rate can be achieved.

Keywords Three-dimensional flow · MHD · Hybrid nanofluid · Convective condition

Introduction

The investigation of boundary layer flow and heat transfer by a stretching surface is essential in engineering and industrial technology. Examples of such flows are in aerodynamics, metallurgy, fluid movies in precipitation process, hot rolling, wire drawing, manufactured filaments and so on. In all these situations, the feature of final item relies upon the friction factor and heat transfer rate. It is frequently supposed in these flows that the surface is linearly stretched, i.e. the velocity of the surface is linearly and directly proportional to the distance from the fixed point. But in real-world, it is not necessary for the stretching sheet to be linear as contended by Gupta and Gupta (1997). For instance, Emmanuel and Khan (2006) considered an exponentially stretching surface. Exponentially stretching surface has more extensive applications for example, in the situation of softening and hardening of copper wires. Khan and Sanjayanand (2005) analytically investigated the flow and heat transfer properties past an exponentially stretching sheet. Nadeem and Lee (2012) wonderfully clarified the characteristics of nanofluid over an exponentially stretching surface.

Majority of the fluids are not good conductors of heat because of their lower thermal conductivity. By using the ordinary heat transfer fluids, cooling rate cannot be enhanced. To adapt up to this issue and to improve heat conductivity or other heat properties of these liquids, a recently created strategy is utilized which includes expansion of nano-sized particles of very good conductors of heat, for example titanium, iron and aluminum to the liquids (Choi 2009). Choi (1995) first introduced the term "nanofluid". Choi et al. (2001) demonstrated that the thermal conductivity of typical liquids can be multiplied by adding nanoparticles to base liquids that likewise fuse other thermal properties. Nanoparticles along with their little volume fraction, stability and remarkable useful applications in optical, biomedical and electronic fields have opened new horizons of research. Recently many scholars have discussed the nanoparticle phenomena in different geometries with pertinent physical properties of fluid, see refs. (Sheikholeslami and Zeeshan 2017; Sheikholeslami and Sadoughi 2018; Sheikholeslami and Shehzad 2018; Hussain et al. 2018; Sheikholeslami et al. 2018a, b, 2019a, b; Sheikholeslami 2018, 2019a, b, c; Sheikholeslami and Seyednezhad 2018).

The recent improvements of carbon nanotubes (CNTs) have reformed the new field of nanotechnology and made extraordinary commitments to both fundamental science and designing. Since hybrid nanofluids are recent development in heat generation fluids, only a few studies have been carried

✉ T. Hayat
t.hayat@math.qau.edu.pk

1 Department of Mathematics, Quaid-i-Azam University, Islamabad, Pakistan

out on their fusion. Lately, some numerical investigations (Nasrin and Alim 2014; Nimmagadda and Venkatasubbaiah 2015; Hayat and Nadeem 2017) were carried out on hybrid nanofluid as a new concept in technology. The measurement of viscosity and thermal conductivity of the Al_2O_3–Cu/H_2O hybrid nanofluid has been conducted by Suresh et al. (2011). They concluded that all the parameters were enhanced with solid volume fraction of nanoparticles. Moghadassi et al. (2015) examined the impact of Al_2O_3–H_2O which was nanofluid and hybrid which comprised Al_2O_3–Cu/H_2O. He depicted that the Al_2O_3–Cu/H_2O (hybrid nanofluid) possess a greater coefficient of heat transfer convention. Sarkar et al. (2015) brought to our knowledge the recent studies in the field of hybrid nanofluids. Tayebi and Chamkha (2016) examined the heat transfer phenomenon inside an annulus with Cu–Al_2O_3/H_2O numerically. The influence of Lorentz force with Hybrid nanofluid has been studied by Devi and Devi (2016).

Magneto-hydrodynamic (MHD) manages the flow of conducting liquids. The uses of MHD spread an extensive variety of physical regions for example, MHD generators and pumps, modern metallurgy, sanitization of unrefined petroleum, optimal design warming, geophysics, plasma material science and liquid beads showers (Sheikholeslami et al. 2018a, b, 2019a, b; Hatami et al. 2014; Sheikholeslami and Ganji 2017; Sheikholeslami and Rokni 2017; Sheikholeslami and Zia 2016; Ellahi et al. 2018; Zeeshan et al. 2018; Fetecau et al. 2018; Hassan et al. 2018; Hussain et al. 2018; Majeed et al. 2018; Alamri et al. 2019). So, our objective here is to improve the properties of single particle nanofluids by introducing hybrid nanofluids which provide great enhancement in thermal properties by considering different aspects.

Momentum and temperature description

We propose the 3D, steady, rotating flow of an electrically conducting hybrid nanofluid over an exponentially stretching surface. The flow coincides with the plane $z = 0$ (see Fig. 1). A uniform magnetic field is applied perpendicular to the surface to see its maximum effects. As carbon nanotubes have high thermal conductivity, we consider nanoparticles of *SWCNT* and *MWCNT* and water as a base fluid. First of all, *MWCNT* (ϕ_1) of 0.1 volume fraction is dispersed into the water to constitute *MWCNT-Water* nanofluid. Further, nanoparticles of *SWCNT* (ϕ_2) are scattered into the *MWCNT-Water* nanofluid to acquire our required hybrid nanofluid. The rotation of the fluid is about z-axis so that the angular velocity of the fluid is constant. Now the transport equations are

$$\nabla . \vec{V} = 0, \tag{1}$$

$$\rho_{\text{hnf}} \frac{d\vec{V}}{dt} + \vec{\Omega} \times \vec{V} = -\nabla p + \left(\mu_{\text{hnf}} \right) \nabla^2 \vec{V} + \vec{j} \times \vec{B}, \tag{2}$$

$$\frac{dT}{dt} = \alpha_{\text{hnf}} \nabla^2 T. \tag{3}$$

where α_{hnf} is thermal diffusivity of hybrid nanofluid, μ_{hnf} is hybrid nanofluid's dynamic viscosity, ρ_{hnf} is the density of hybrid nanofluid, k_{hnf} is the thermal conductivity of hybrid nanofluid, $\left(\rho C_p \right)_{\text{hnf}}$ is the heat capacity of hybrid nanofluid and ϕ is the nanoparticle's volume fraction which is defined as follows:

Fig. 1 Schematic diagram of the model
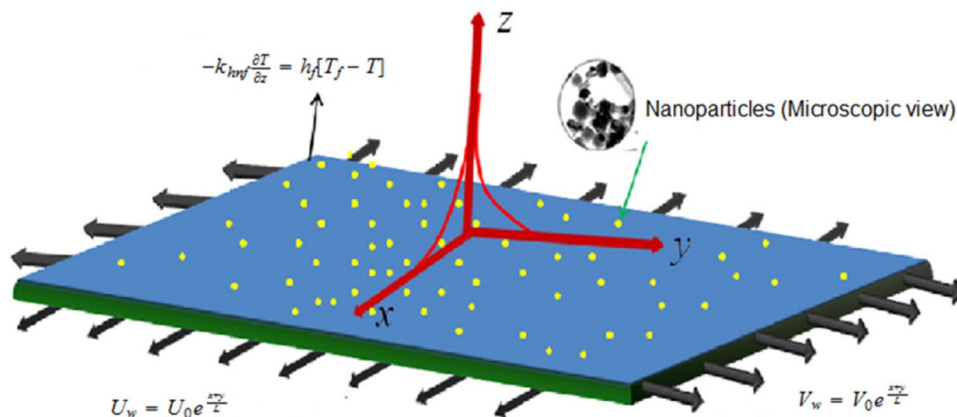
$$\alpha_{\text{hnf}} = \frac{k_{\text{hnf}}}{(\rho c_p)_{\text{hnf}}}, \; \mu_{\text{hnf}} = \frac{\mu_f}{(1-\phi_1)^{2.5}(1-\phi_2)^{2.5}},$$

$$\rho_{\text{hnf}} = \left[(1-\phi_2)\left\{(1-\phi_1)\rho_f + \phi_1\rho_{s_1}\right\} + \phi_2\rho_{s_2}\right],$$

$$(\rho C_p)_{\text{hnf}} = \left[(1-\phi_2)\left\{(1-\phi_1)(\rho C_p)_f + \phi_1(\rho C_p)_{s_1}\right\} + \phi_2(\rho C_p)_{s_2}\right],$$

$$\frac{k_{\text{hnf}}}{k_{\text{nf}}} = \frac{(k_{s_2} + 2k_{\text{nf}}) - 2\phi_2(k_{\text{nf}} - k_{s_2})}{(k_{s_2} + 2k_{\text{nf}}) + \phi_2(k_{\text{nf}} - k_{s_2})}, \; \frac{k_{\text{nf}}}{k_f} = \frac{(k_{s_1} + 2k_f) - 2\phi_1(k_f - k_{s_1})}{(k_{s_1} + 2k_f) + \phi_1(k_f - k_{s_1})},$$

$$\nu_{\text{hnf}} = \frac{\mu_{\text{hnf}}}{\rho_{\text{hnf}}}, \; \Omega = \Omega_0 e^{\frac{x+y}{L}}. \tag{4}$$

After applying boundary layer approximation, we are left with the following equations (Hayat and Nadeem 2018; Hayat et al. 2018):

Continuity equation

$$\left[\frac{\partial u}{\partial x} + \frac{\partial v}{\partial y} + \frac{\partial w}{\partial z}\right] = 0, \tag{5}$$

Momentum equations

$$\left[u\frac{\partial u}{\partial x} + v\frac{\partial u}{\partial y} + w\frac{\partial u}{\partial z} - 2\Omega v\right] = \frac{\mu_{\text{hnf}}}{\rho_{\text{hnf}}}\frac{\partial^2 u}{\partial z^2} - \frac{\sigma B_0^2 u}{\rho_{\text{hnf}}}, \tag{6}$$

$$\left[u\frac{\partial v}{\partial x} + v\frac{\partial v}{\partial y} + w\frac{\partial v}{\partial z} + 2\Omega u\right] = \frac{\mu_{\text{hnf}}}{\rho_{\text{hnf}}}\frac{\partial^2 v}{\partial z^2} - \frac{\sigma B_0^2 v}{\rho_{\text{hnf}}}. \tag{7}$$

Energy equation

$$u\frac{\partial T}{\partial x} + v\frac{\partial T}{\partial y} + w\frac{\partial T}{\partial z} = \alpha_{\text{hnf}}\left(\frac{\partial^2 T}{\partial z^2}\right) \tag{8}$$

Boundary conditions

$$\left. \begin{array}{l} u = u_w, \; v = v_w, \; -k_{\text{hnf}}\frac{\partial T}{\partial z} = h_f(T_w - T), \text{ at } z = 0, \\ u \to 0, \; v \to 0, \; T \to T_\infty, \text{ as } z \to \infty. \end{array} \right\} \tag{9}$$

Stretching velocities at surface and temperature at the wall are defined as follows:

$$u_w = u_0 e^{\frac{x+y}{L}}, v_w = v_0 e^{\frac{x+y}{L}}, T_w = T_\infty + T_0 e^{\frac{A(x+y)}{2L}} \tag{10}$$

Using suitable similarity transformations given below,

$$\left. \begin{array}{l} u = u_0 e^{\frac{x+y}{L}} p'(\eta), v = u_0 e^{\frac{x+y}{L}} q'(\eta), w = -\left(\frac{\nu u_0}{2L}\right)^{\frac{1}{2}} e^{\frac{x+y}{2L}}\{p + \eta p' + q + \eta q'\}, \\ T = T_\infty + T_0 e^{\frac{A(x+y)}{2L}} f(\eta), \eta = \left(\frac{u_0}{2\nu L}\right)^{\frac{1}{2}} e^{\frac{x+y}{2L}} z. \end{array} \right\} \tag{11}$$

After applying the above similarity transformations on Eqs. (5–9), the continuity equation is identically satisfied while momentum and energy equations take the following form:

$$\frac{\rho_f}{\rho_{\text{hnf}}}(A_1(\phi))p''' + p''(p+q) - 2p'(p'+q') + 4\gamma g' - 2M\frac{\rho_f}{\rho_{\text{hnf}}}p' = 0, \tag{12}$$

$$\frac{\rho_f}{\rho_{\text{hnf}}}(A_1(\phi))q''' + q''(p+q) - 2q'(p'+q') - 4\gamma p' - 2M\frac{\rho_f}{\rho_{\text{hnf}}}q' = 0, \tag{13}$$

$$\frac{1}{\text{Pr}}\frac{(k_{\text{hnf}}/k_f)f''}{\left[(1-\phi_2)\left\{(1-\phi_1) + \phi_1\frac{(\rho C_p)_{s_1}}{(\rho C_p)_f}\right\} + \phi_2\frac{(\rho C_p)_{s_2}}{(\rho C_p)_f}\right]}$$
$$- A(p'+q')f + (p+q)f' = 0 \tag{14}$$

The associated boundary conditions are

$$\left. \begin{array}{l} p(0) = 0, p'(0) = 1, q(0) = 0, \\ q'(0) = \alpha, f'(0) = -\text{Nc}\left(\frac{k_f}{k_{\text{hnf}}}\right)(1-f(0)), \text{ as } \eta \to 0, \\ p' \to 0, q' \to 0, f \to 0, \text{ as } \eta \to \infty. \end{array} \right\} \tag{15}$$

where $\gamma, M, \alpha, \text{Nc}$ and Pr signify rotation parameter, Hartmann number, stretching ratio parameter, convective parameter and Prandtl number, respectively, and they are defined as follows:

$$\left. \begin{array}{l} \gamma = \frac{\Omega_0 L}{u_0}, A_1(\phi) = \frac{\mu_{\text{hnf}}}{\mu_f} = \frac{1}{(1-\phi_1)^{2.5}(1-\phi_2)^{2.5}}, \alpha = \frac{v_0}{u_0}, \\ M = \frac{\sigma B_0^2 L}{\rho_f u_0} e^{-\left(\frac{x+y}{L}\right)}, \text{Nc} = \frac{h_f}{k_f}\sqrt{\frac{2\nu_f L}{u_0}} e^{-\left(\frac{x+y}{2L}\right)}, \text{Pr} = \frac{(\mu C_p)_f}{k_f}. \end{array} \right\} \tag{16}$$

Further, the skin friction coefficients and Nusselt number can be defined as (Rao et al. 2015):

$$C_{\text{fx}} = \frac{\tau_{\text{wx}}}{\frac{1}{2}\rho_f u_w^2}, \, C_{\text{fy}} = \frac{\tau_{\text{wy}}}{\frac{1}{2}\rho_f u_w^2}, \text{Nu}_x = \frac{xQ_w}{k_f\left(T_w - T_\infty\right)}, \quad (17)$$

where τ_{wx}, τ_{wy} and Q_w are shear stresses at the surface along two lateral directions and heat flux at the surface, defined as follows:

$$\tau_{\text{wx}} = \mu_{\text{hnf}}\left(\frac{\partial u}{\partial z}\right)_{z=0}, \, \tau_{\text{wy}} = \mu_{\text{hnf}}\left(\frac{\partial v}{\partial z}\right)_{z=0}, \, Q_w = -k_{\text{hnf}}\left(\frac{\partial T}{\partial z}\right)_{z=0}. \Bigg\} \tag{18}$$

The non-dimensional form after simplification is

$$\left.\begin{array}{l} \frac{1}{\sqrt{2}}C_{\text{fx}}\left(\text{Re}_x\right)^{\frac{1}{2}} = A_1^{-1}p''(0), \, \frac{1}{\sqrt{2}}C_{\text{fy}}\left(\text{Re}_y\right)^{\frac{1}{2}} = A_1^{-1}q''(0), \\ \sqrt{2}\frac{L}{x}\text{Nu}_x\text{Re}^{-\frac{1}{2}} = -\frac{k_{\text{hnf}}}{k_f}f'(0). \end{array}\right\} \tag{19}$$

Numerical scheme

The coupled non-linear ordinary differential Eqs. (12–14) along with boundary conditions (15) are first converted into first order and are then solved numerically using BVP-4C technique (Shampine et al. 2000, 2003; Nadeem et al. 2019). The implicit MATLAB library bvp4c for boundary value problem executes 3-stage Lobatto IIIA formula. Due to their great stability properties, Lobatto IIIA method has been assumed for boundary value problems (BVP). The procedure of this technique is as follows:

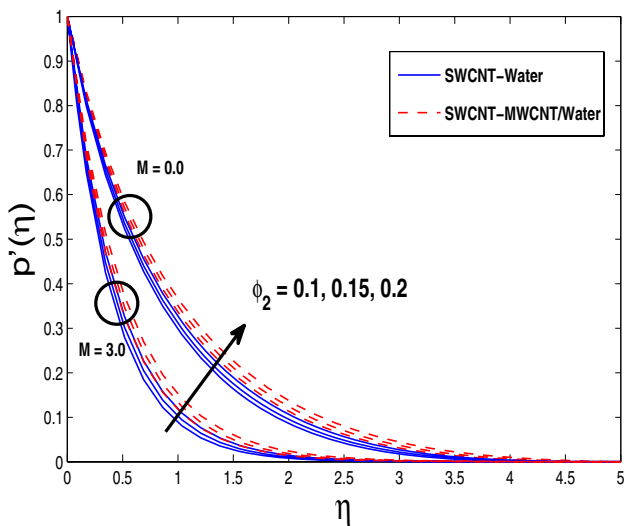$$p = y_1, p' = y_2, p'' = y_3, q = y_4, q' = y_5, q'' = y_6, f = y_7, f' = y_8, \tag{20}$$
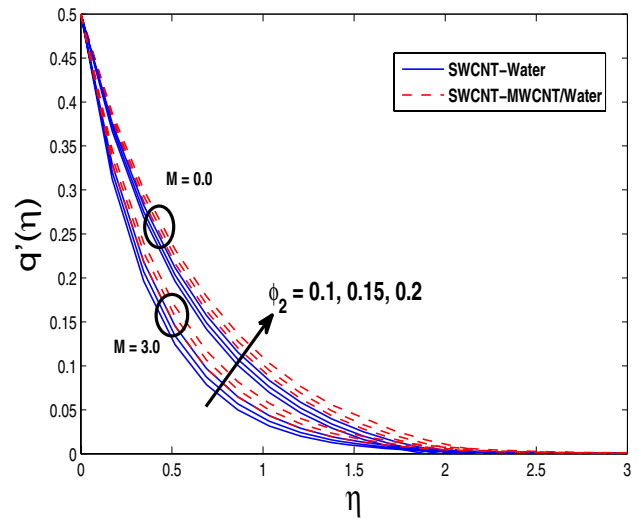

Fig. 3 Impact of ϕ_2 on $q'(\eta)$

$$\left.\begin{array}{l} y_3' = \frac{\mu_f}{\mu_{\text{hnf}}}\frac{\rho_{\text{hnf}}}{\rho_f}\left(2y_2(y_2 + y_5) - y_3(y_1 + y_4) - 4\gamma y_5\right) + 2\frac{\mu_f}{\mu_{\text{hnf}}}My_2, \\ y_6' = \frac{\mu_f}{\mu_{\text{hnf}}}\frac{\rho_{\text{hnf}}}{\rho_f}\left(2y_5(y_2 + y_5) - y_6(y_1 + y_4) - 4\gamma y_2\right) + 2\frac{\mu_f}{\mu_{\text{hnf}}}My_5, \\ y_8' = \left(\frac{k_f}{k_{\text{hnf}}}\right)\frac{(\rho C_p)_{\text{hnf}}}{(\rho C_p)_f}\text{Pr}\,A(y_1 + y_4)y_7 - (y_2 + y_5)y_8, \end{array}\right\} \tag{21}$$

with boundary conditions

$$\left.\begin{array}{l} y_1(0) = 0, y_2(0) = 1, y_4(0) = 0, y_5(0) = \alpha, \\ y_8(0) = -\text{Nc}\frac{k_f}{k_{\text{hnf}}}\left(1 - y_7(0)\right), y_2(10) = 0, \\ y_5(10) = 0, y_7(10) = 0. \end{array}\right\} \tag{22}$$

Fig. 2 Impact of ϕ_2 on $p'(\eta)$
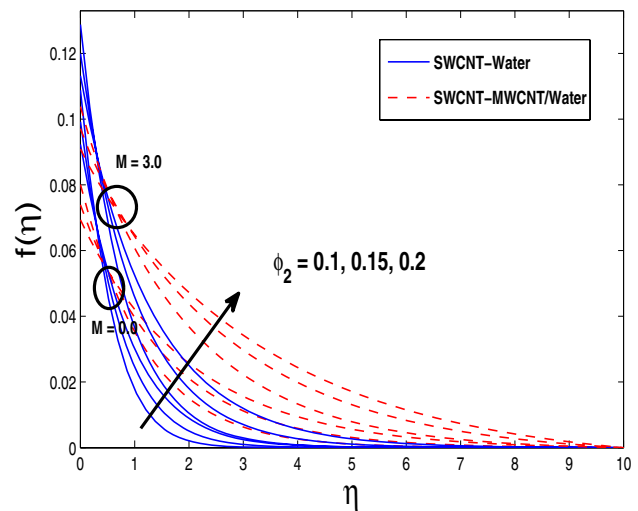
Fig. 4 Impact of ϕ_2 on $f(\eta)$
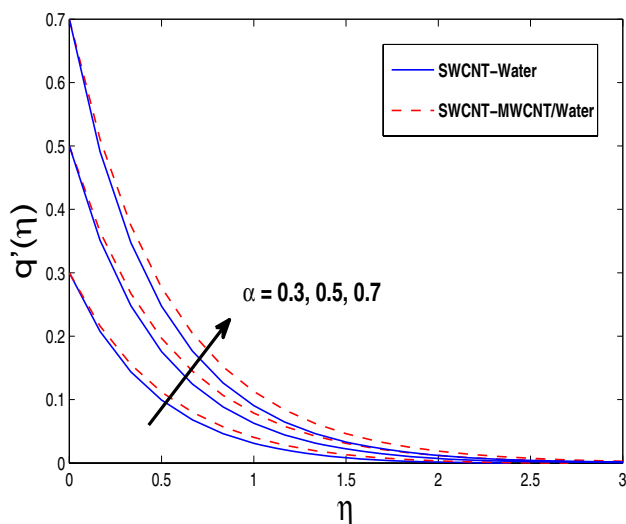
Fig. 5 Impact of α on $q'(\eta)$
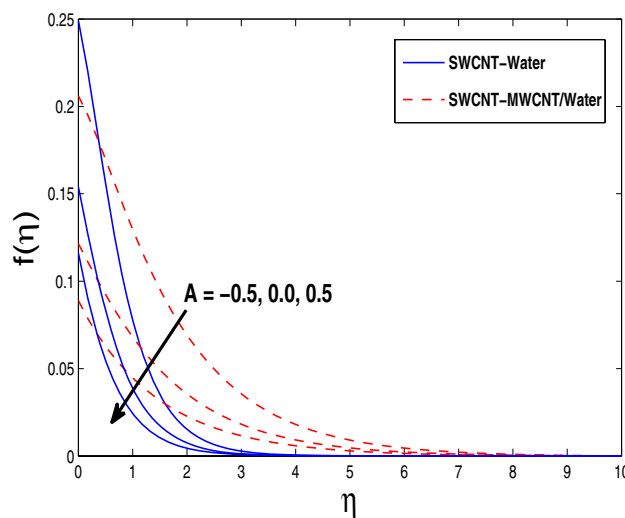

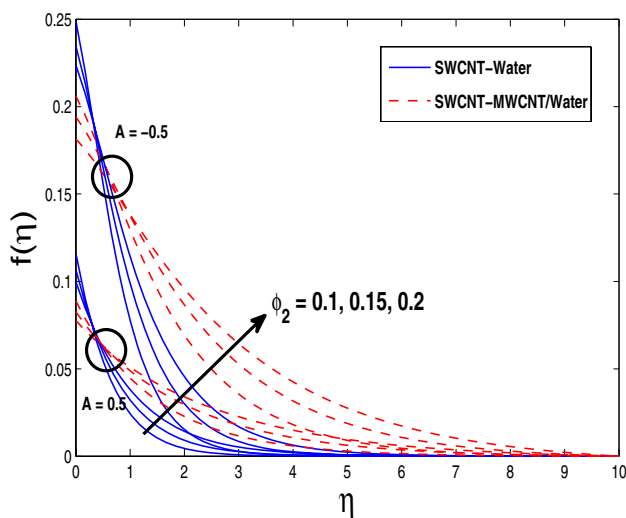**Fig. 7** Impact of A on $f(\eta)$

Fig. 6 Impact of ϕ_2 on $f(\eta)$
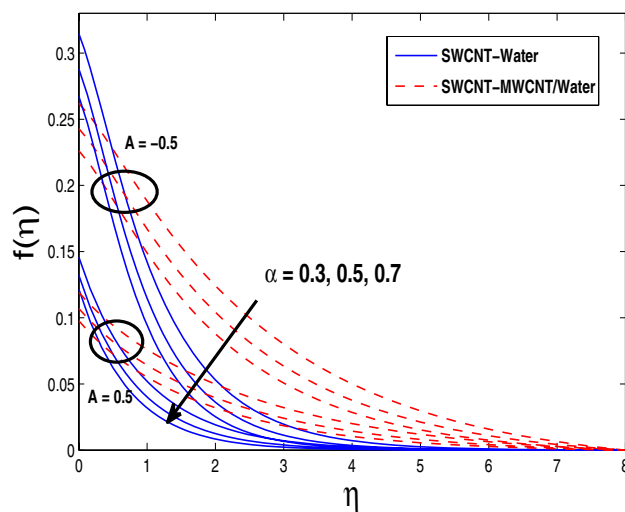

Fig. 8 Impact of α on $f(\eta)$

Now the above system is reduced to first-order ordinary differential equations and then this method is repeated until the criterion of 10^{-6} is achieved. The solutions represent main characteristics of the problem which is analyzed graphically and in tabular form.

Graphical outcomes

See Figs. 2, 3, 4, 5, 6, 7, 8, 9, 10, 11, 12, 13, 14, 15, 16, 17, 18.

Results and discussion

We have examined in this section the velocity distribution in two lateral directions ($p'(\eta)$, $q'(\eta)$) and temperature distribution $f(\eta)$ for different pertinent parameters such as nanoparticle volume fraction ϕ_2, Hartmann number M, rotation parameter γ, stretching ratio α, temperature exponent A and convective parameter Nc. The impact of ϕ_2 and Hartmann number M on velocities ($p'(\eta)$, $q'(\eta)$) and temperature distribution $f(\eta)$ is portrayed in Figs. 2, 3, 4. It is observed that velocity and temperature distribution increases for increasing values of ϕ_2. The reason behind that is, as ϕ_2 increases, the thermal conductivity of both nanofluid *SWCNT-Water* and hybrid nanofluid *SWCNT-MWCNT/Water* amplifies and
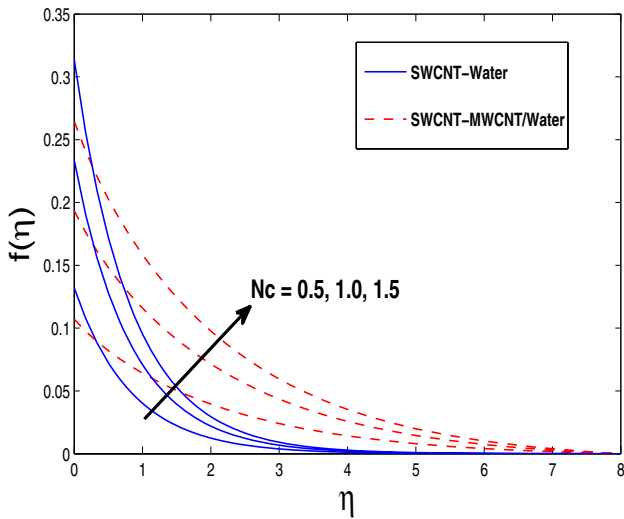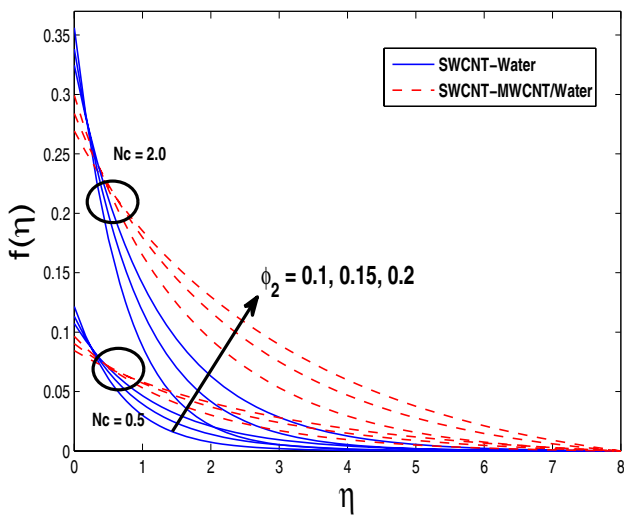
Fig. 9 Impact of Nc on $f(\eta)$

Fig. 11 Impact of skin friction along x axis with M and γ

Fig. 10 Effect of ϕ_2 on $f(\eta)$
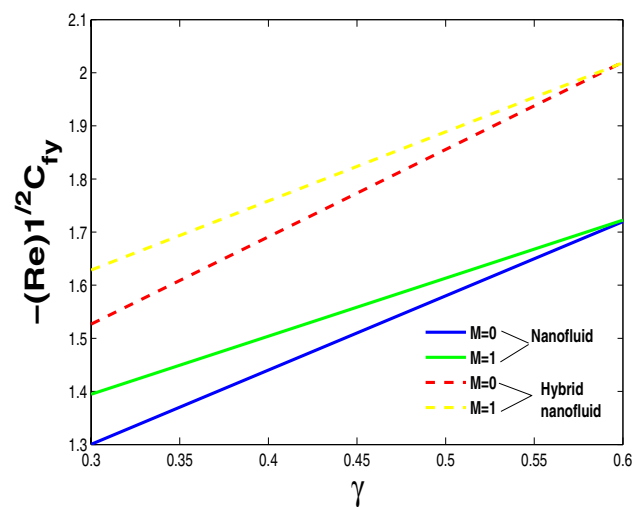
Fig. 12 Impact of skin friction along y axis with M and γ

that is why velocity and temperature profile increases. But M has the opposite impact on momentum and temperature profiles. The increasing value of Hartmann number M decreases the liquid velocity in both directions but enhances the temperature profile $f(\eta)$. Physically, magnetic field is used to control the flow behavior. It creates Lorentz force which is the resistive force and restricts the motion of the fluid. That is why liquid velocity decreases.

Figure 5 elucidates the effects of stretching ratio α on y component of velocity profile $q'(\eta)$. Here one can observe that fluid velocity enhances with stretching ratio α. The impact of ϕ_2 on temperature profile $f(\eta)$ is explored in Fig. 6. From this figure it is evident that temperature profile $f(\eta)$ rises for any under consideration value of A with the elevation in nanoparticle volume fraction ϕ_2. Figure 7
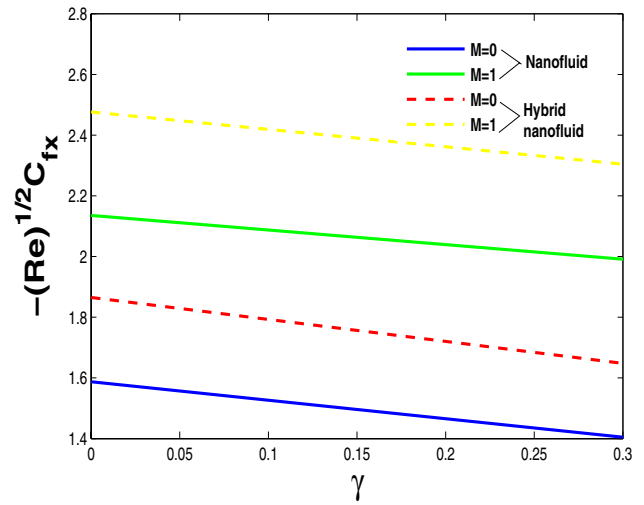
demonstrates the behavior of temperature exponent A on temperature profile $f(\eta)$. Here one can observe that temperature exponent A is the decreasing function of temperature profile $f(\eta)$ for both nanofluid *SWCNT-Water* and hybrid nanofluid *SWCNT-MWCNT/Water*.

Figures 8 and 9 are sketched to depict the variation of α and Nc on temperature profile $f(\eta)$. An elevation in stretching ratio α reduces the temperature as observed through Fig. 8. From Fig. 9, it is illustrated that there is a remarkable raise in temperature for both nanofluid *SWCNT-Water* and hybrid nanofluid *SWCNT-MWCNT/Water* with the elevation in convective parameter Nc. But from figure it is obvious that nanofluid *SWCNT-Water* has a lower temperature as compared to hybrid nanofluid *SWCNT-MWCNT/Water*. Physically, as Nc enhances, the
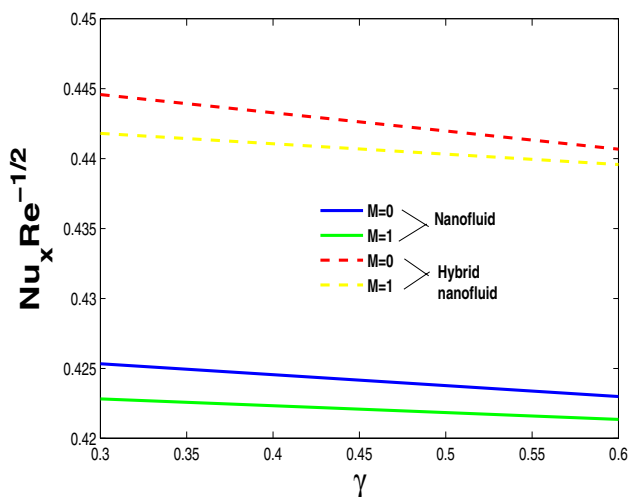
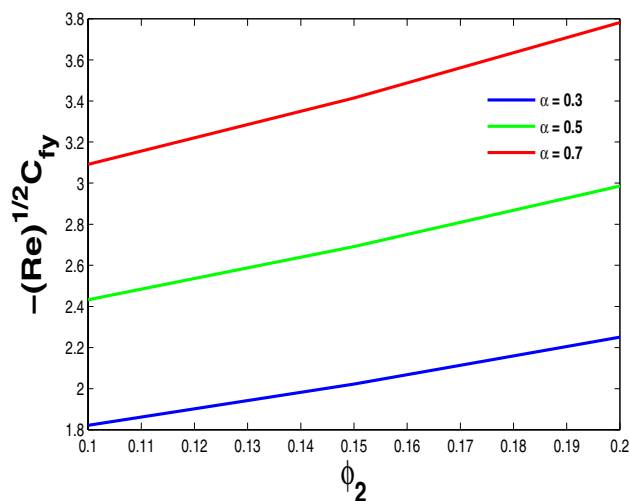**Fig. 13** Impact of local Nusselt number with M and γ

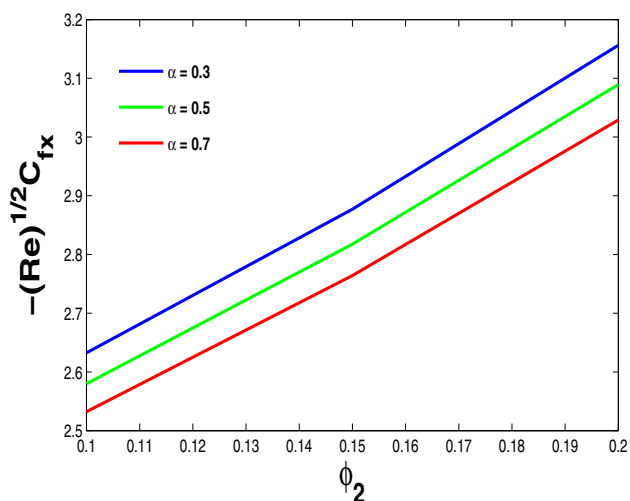**Fig. 15** Impact of skin friction along y axis with α and ϕ_2

Fig. 14 Impact of skin friction along x axis with α and ϕ_2
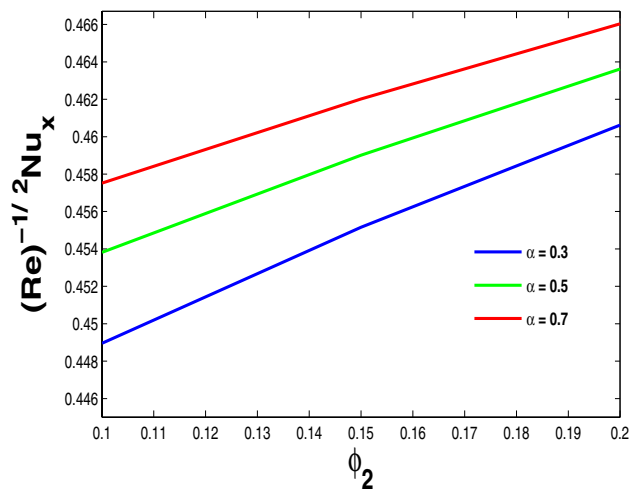

Fig. 16 Impact of local Nusselt number with α and ϕ_2

lower surface of the stretching sheet gets heated by the hot fluid which leads to convective heat transfer. Hence the temperature distribution increases. Figure 10 demonstrates the impact of nanoparticle volume fraction ϕ_2 and convective parameter Nc on temperature profile $f(\eta)$. Larger values of convective parameter Nc with the raise in nanoparticle volume fraction ϕ_2 correspond to higher temperature profile $f(\eta)$. Now we examine the behavior of various physical parameters for both nanofluid *SWCNT-Water* and hybrid nanofluid *SWCNT-MWCNT/Water* on skin friction coefficients (C_{fx}, C_{fy}) and local Nusselt number Nu$_x$ through Figs. 11, 12, 13, 14, 15, 16, 17, 18. The nature of M and γ on C_{fx} is displayed in Fig. 11. It is observed that as we enhance the Hartmann number M, the skin friction amplifies but it decreases with rotation parameter γ.

The enhancement in skin friction is due to the increase in Lorentz force which resists the motion of the fluid. As a result, the viscosity of the fluid increases and that is why C_{fx} increases. Figure 12 elucidates the effect of M and γ on y component of skin friction. Here we observe that skin friction along y direction increases with both M and γ. Figure 13 portrays the nature of Hartmann number M and rotation parameter γ on the local Nusselt number. From figure it is clear that the rate of heat transfer decreases with both Hartmann number M and rotation parameter γ. Here we observe that even in the presence of Hartmann number and rotation parameter, the rate of heat transfer of hybrid nanofluid *SWCNT-MWCNT/Water* is higher than simple nanofluid *SWCNT-Water*.
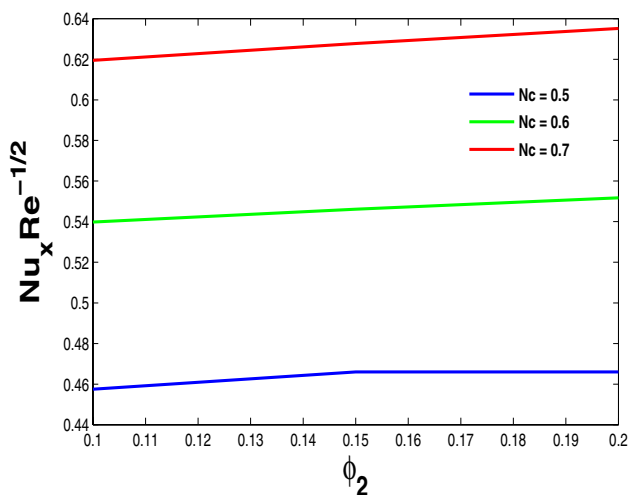
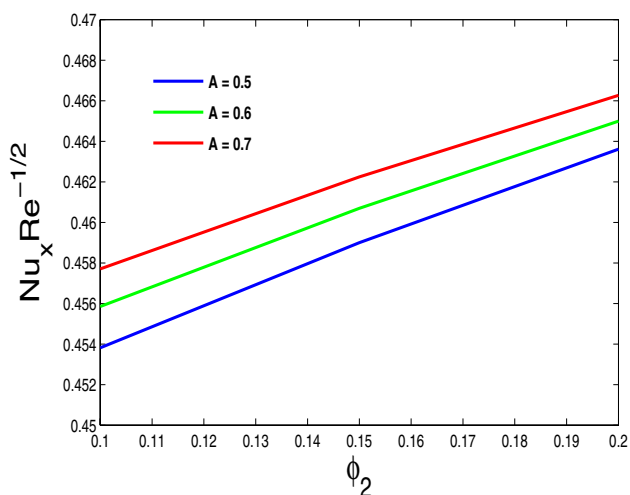**Fig. 17** Impact of local Nusselt number with Nc and ϕ_2

Fig. 18 Impact of local Nusselt number with A and ϕ_2

Table 1 Thermophysical properties of carbon nanotubes and base fluid

Thermophysical properties	MWCNT	SWCNT	Water
ρ (kg/m³)	1600	2600	997.1
C_p (j/kg)K	796	425	4179
k (W/mK)	3000	6600	0.613

Figures 14, 15 and 16 describe the behavior of stretching ratio α and ϕ_2 on skin friction coefficients along two lateral directions (C_{fx}, C_{fy}) and the local Nusselt number Nu$_x$. Here, C_{fx} decreases with the α, but C_{fy} and rate of heat transfer enhance with α. In each figure, the friction factor and heat transfer rate increase with carbon nanotubes' volume fraction ϕ_2. This is due to the reason that thermal conductivity of hybrid nanofluid *SWCNT-MWCNT/*Water intensifies with the increase in carbon nanotube volume fraction ϕ_2. As seen in Fig. 17, there is magnificent increase in the rate of heat transfer with the rise in even small values of convective parameter Nc. Figure 18 shows the variation of ϕ_2 and temperature exponent A on the rate of heat transfer. Here one can observe that the rate of heat transfer amplifies with temperature exponent A and ϕ_2. The thermo-physical properties of carbon nanotubes and base fluid are illustrated in Table 1. The effects of pertinent physical parameters such as Hartmann number (M), stretching ratio (α), rotation parameter (γ), temperature exponent (A), convective parameter (Nc) and nanoparticle volume fraction (ϕ_2) on skin friction coefficients (C_{fx}, C_{fy}) and the local Nusselt number Nu$_x$ are presented in Table 2 where Table 3 represent the comparison table shows a good agreement which previous published data.

Key points

To examine the three-dimensional magneto hydrodynamic flow of hybrid nanofluid in the presence of CNTs along an exponentially stretching surface, a numerical analysis is executed. Impact of relevant physical parameters on two lateral velocities, temperature distribution, friction factor as well as on the rate of heat transfer are discussed in comprehensive form. The conclusion of present research is listed as follows:

- Addition of ϕ_2 escalates the velocity, temperature, friction factor and heat transfer rate.
- The flow of hybrid nanofluid plays a noteworthy part in heat transfer in the presence of magnetic field.
- The rate of heat transfer increases with stretching ratio parameter, convective parameter and temperature exponent.
- Hartmann number increases the friction factor but decreases the rate of heat transfer.
- The temperature along with thermal boundary layer thickness escalates by adding solid volume fraction.
- Enhancing the temperature exponent decreases the temperature profile.
- It is noted that hybrid nanofluid gives significant heat transfer performance as compared to simple nanofluid.

Table 2 Impact of Hartmann number (M), stretching ratio parameter (α), rotation parameter (γ), temperature exponent (A), convective parameter (Nc) and nanoparticle volume fraction (ϕ_2) on skin friction coefficient and local Nusselt number

M	Wang	γ	A	Nc	ϕ_2	C_{fx}	C_{fy}	$-f''(0)$
0						1.99143	1.84435	0.45842
1	0.5	0.3	0.5	0.5	0.1	2.70152	1.94645	0.45623
2						3.26799	2.11902	0.4538
	0.0					2.61565	0.525887	0.44446
1	0.5	0.3	0.5	0.5	0.1	2.70152	1.94645	0.45623
	1.0					2.7860	3.66727	0.46278
		0.0				2.91478	1.45739	0.45764
1	0.5	0.3	0.5	0.5	0.1	2.70152	1.94645	0.45623
		0.6				2.57977	2.43254	0.45382
						2.70152	1.94645	0.44199
1	0.5	0.3	0.0	0.5	0.1	2.70152	1.94645	0.45623
			0.5			2.70152	1.94645	0.4643
			1.0					
				0.5		2.70152	1.94645	0.45623
1	0.5	0.3	0.5	1.0	0.1	2.70152	1.94645	0.839
				1.5		2.70152	1.94645	1.1647
1	0.5	0.3	0.5	0.5	0.1	2.70152	1.94645	0.45623
					0.15	2.95087	2.14545	0.46107
					0.2	3.23549	2.37213	0.46532

Table 3 Comparison of $-p''(0)$ for various values of stretching parameter α when $\gamma = \phi_1 = \phi_2 = 0$

α	Wang (1984)	Ariel (2007)	Butt and Ali (2015)	Present results
0.0	1	1	1	1
0.1	1.020902	1.017027	1.020260	1.02137
0.2	1.041804	1.034587	1.039495	1.0404
0.3	1.062705	1.052470	1.057955	1.05871
0.4	1.083607	1.070529	1.075788	1.07643
0.5	1.104509	1.088662	1.093095	1.09364

References

Alamri SZ, Khan AA, Azeez M, Ellahi R (2019) Effects of mass transfer on MHD second grade fluid towards stretching cylinder: a novel perspective of Cattaneo–Christov heat flux model. Phys Lett A 383:276–281

Ariel PD (2007) The three-dimensional flow past a stretching sheet and the homotopy perturbation method. Comput Math Appl 54:920–925

Butt AS, Ali A (2015) Investigation of entropy generation effects in magnetohydrodynamic three-dimensional flow and heat transfer of viscous fluid over a stretching surface. J Braz Soc Mech Sci Eng 37:211–219

Choi SUS (1995) Enhancing conductivity of fluids with nanoparticles, ASME Fluid Eng. Division 231:99–105

Choi SUS (2009) Nanofluids: from vision to reality through research. J Heat Transfer 131:33106

Choi SU, Zhang ZG, Yu W, Lockwood FE, Grulke EA (2001) Anomalously thermal conductivity enhancement in nanotube suspensions. Appl Phys Lett 79:2252–2254

Devi SSU, Devi SPA (2016) Numerical investigation of three-dimensional hybrid Cu–Al$_2$O$_3$/water nanofluid flow over a stretching sheet with effecting Lorentz force subject to Newtonian heating. Can J Phys 94:490–496

Ellahi R, Alamri SZ, Basit A, Majeed A (2018) Effects of MHD and slip on heat transfer boundary layer flow over a moving plate based on specific entropy generation. J Taibah Univ Sci 12:476–482

Emmanuel S, Khan SK (2006) On heat and mass transfer in a viscoelastic boundary layer flow over an exponentially stretching sheet. Int J Therm Sci 45:819–828

Fetecau C, Ellahi R, Khan M, Shah NA (2018) Combined porous and magnetic effects on some fundamental motions of Newtonian fluids over an infinite plate. J Porous Media. https://doi.org/10.1615/JPorMedia.v21.i7.20

Gupta PS, Gupta AS (1997) Heat and mass transfer on a stretching sheet with suction or blowing. Can J Chem Eng 55(6):744–746

Hassan M, Marin M, Alsharif A, Ellahi R (2018) Convective heat transfer flow of nanofluid in a porous medium over wavy surface. Phys Lett A 382:2749–2753

Hatami M, Hosseinzadeh K, Domairry G, Behnamfar MT (2014) Numerical study of MHD two-phase Couette flow analysis for fluid-particle suspension between moving parallel plates. J Taiwan Inst Chem Eng 45:2238–2245

Hayat T, Nadeem S (2017) Heat transfer enhancement with Ag–CuO/water hybrid nanofluid. Results Phys 7:2317–2324

Hayat T, Nadeem S (2018) An improvement in heat transfer for rotating flow of hybrid nanofluid: a numerical study. Can J Phys 96:1420–1430

Hayat T, Nadeem S, Khan AU (2018) Numerical analysis of Ag–CuO/water rotating Hybrid nanofluid with heat generation/absorption. Can J Phys. https://doi.org/10.1139/cjp-2018-0011

Hussain F, Ellahi R, Zeeshan A (2018) Mathematical models of electro-magnetohydrodynamic multiphase flows synthesis with nanosized hafnium particles. Appl Sci 8:275

Khan SK, Sanjayanand E (2005) Viscoelastic boundary layer flow and heat transfer over an exponential stretching sheet. Int J Heat Mass

Transf 48:1534–1542. https://doi.org/10.1016/J.IJHEATMASS TRANSFER.2004.10.032

Majeed A, Zeeshan A, Alamri SZ, Ellahi R (2018) Heat transfer analysis in ferromagnetic viscoelastic fluid flow over a stretching sheet with suction. Neural Comput Appl 30:1947–1955

Moghadassi A, Ghomi E, Parvizian F (2015) A numerical study of water based Al_2O_3 and Al_2O_3–Cu hybrid nanofluid effect on forced convective heat transfer. Int J Therm Sci 92:50–57

Nadeem S, Lee C (2012) Boundary layer flow of nanofluid over an exponentially stretching surface. Nanoscale Res Lett 7:94

Nadeem S, Hayat T, Khan AU (2019) Numerical study on 3D rotating hybrid SWCNT-MWCNT flow over a convectively heated stretching surface with heat generation/absorption. Phys Scr (accepted)

Nasrin R, Alim MA (2014) Finite element simulation of forced convection in a flat plate solar collector: influence of nanofluid with double nanoparticles. J Appl Fluid Mech 7:543–556

Nimmagadda R, Venkatasubbaiah K (2015) Conjugate heat transfer analysis of micro-channel using novel hybrid nanofluids ($Al_2O_3^+$ Ag/Water). Eur J Mech 52:19–27

Rao JA, Vasumathi G, Mounica J (2015) Joule heating and thermal radiation effects on MHD boundary layer flow of a nanofluid over an exponentially stretching sheet in a porous medium. World J Mech 5:151

Sarkar J, Ghosh P, Adil A (2015) A review on hybrid nanofluids: recent research, development and applications. Renew Sustain Energy Rev 43:164–177

Shampine LF, Kierzenka J, Reichelt MW (2000) Solving boundary value problems for ordinary differential equations in MATLAB with bvp4c. Tutor Notes 75275:1–27

Shampine LF, Gladwell I, Shampine L, Thompson S (2003) Solving ODEs with matlab. Cambridge University Press, Cambridge

Sheikholeslami M (2018) Influence of magnetic field on Al2O3-H2O nanofluid forced convection heat transfer in a porous lid driven cavity with hot sphere obstacle by means of LBM. J Mol Liq 263:472–488

Sheikholeslami M (2019a) Numerical approach for MHD Al2O3-water nanofluid transportation inside a permeable medium using innovative computer method. Comput Methods Appl Mech Eng 344:306–318. https://doi.org/10.1016/J.CMA.2018.09.042

Sheikholeslami M (2019b) New computational approach for exergy and entropy analysis of nanofluid under the impact of Lorentz force through a porous media. Comput Methods Appl Mech Eng 344:319–333. https://doi.org/10.1016/J.CMA.2018.09.044

Sheikholeslami M (2019c) New computational approach for exergy and entropy analysis of nanofluid under the impact of Lorentz force through a porous media. Comput Methods Appl Mech Eng 344:319–333

Sheikholeslami M, Ganji DD (2017) Numerical approach for magnetic nanofluid flow in a porous cavity using CuO nanoparticles. Mater Des 120:382–393

Sheikholeslami M, Rokni HB (2017) Simulation of nanofluid heat transfer in presence of magnetic field: a review. Int J Heat Mass Transf 115:1203–1233

Sheikholeslami M, Sadoughi MK (2018) Simulation of CuO-water nanofluid heat transfer enhancement in presence of melting surface. Int J Heat Mass Transf 116:909–919

Sheikholeslami M, Seyednezhad M (2018) Simulation of nanofluid flow and natural convection in a porous media under the influence of electric field using CVFEM. Int J Heat Mass Transf 120:772–781. https://doi.org/10.1016/J.IJHEATMASSTRANS FER.2017.12.087

Sheikholeslami M, Shehzad SA (2018) Numerical analysis of Fe_3O_4–H_2O nanofluid flow in permeable media under the effect of external magnetic source. Int J Heat Mass Transf 118:182–192

Sheikholeslami M, Zeeshan A (2017) Analysis of flow and heat transfer in water based nanofluid due to magnetic field in a porous enclosure with constant heat flux using CVFEM. Comput Methods Appl Mech Eng 320:68–81

Sheikholeslami M, Zia QM (2016) Ellahi R Influence of induced magnetic field on free convection of nanofluid considering Koo-Kleinstreuer-Li (KKL) correlation. Appl Sci 6:324

Sheikholeslami M, Jafaryar M, Li Z (2018a) Second law analysis for nanofluid turbulent flow inside a circular duct in presence of twisted tape turbulators. J Mol Liq 263:489–500

Sheikholeslami M, Shehzad SA, Li Z, Shafee A (2018b) Numerical modeling for alumina nanofluid magnetohydrodynamic convective heat transfer in a permeable medium using Darcy law. Int J Heat Mass Transf 127:614–622

Sheikholeslami M, Gerdroodbary MB, Moradi R et al (2019a) Application of Neural Network for estimation of heat transfer treatment of Al_2O_3–H_2O nanofluid through a channel. Comput Methods Appl Mech Eng 344:1–12. https://doi.org/10.1016/J.CMA.2018.09.025

Sheikholeslami M, Haq R, Shafee A, Li Z (2019b) Heat transfer behavior of nanoparticle enhanced PCM solidification through an enclosure with V shaped fins. Int J Heat Mass Transf 130:1322–1342. https://doi.org/10.1016/J.IJHEATMASSTRANSFER.2018.11.020

Suresh S, Venkitaraj KP, Selvakumar P, Chandrasekar M (2011) Synthesis of Al_2O_3–Cu/water hybrid nanofluids using two step method and its thermo physical properties. Colloids Surf A Physicochem Eng Asp 388:41–48

Tayebi T, Chamkha AJ (2016) Free convection enhancement in an annulus between horizontal confocal elliptical cylinders using hybrid nanofluids. Numer Heat Transf Part A Appl 70:1141–1156

Wang CY (1984) The three-dimensional flow due to a stretching flat surface. Phys Fluids 27:1915–1917

Zeeshan A, Ijaz N, Abbas T, Ellahi R (2018) The sustainable characteristic of bio-bi-phase flow of peristaltic transport of MHD Jeffrey fluid in the human body. Sustainability 10:2671

Springer